PHYSOR-2006, ANS Topical Meeting on Reactor Physics
Organized and hosted by the Canadian Nuclear Society. Vancouver, BC, Canada. 2006 September 10-14

Adaptive automated solution of the multi-group diffusion equations

Yaqi Wang, Jean C. Ragusa[1]
Texas A&M University, Dept. of Nuclear Engineering
129 Zachry Engineering Center, College Station, TX 77843-3133, USA

Abstract

This paper presents fully automated *hp*-refinement strategies applied to multigroup diffusion equations. Exponential convergence rates are achieved for a fraction of the number of unknowns needed with uniform refinement and *h*-refinement strategies. Innovative results include (i) the treatment of adaptivity in the context of the multigroup equations, and, (ii) the definition of a mesh adaptation strategy in the context of eigenvalue outer iterations and thermal iterations.

KEYWORDS: hp-adaptation, mesh refinement, multigroup diffusion

1. Introduction

Computing with high spatial resolution **accurate** and **converged** solutions of the neutron balance equation is a challenging yet important task. The issue of obtaining a solution converged to a desired (i.e., user-prescribed) tolerance is seldom addressed. "Brute force" uniform mesh refinement to answer this issue is not a credible remedy because (1) this process soon comes to a halt due to the enormous increase in the number of unknowns, and, (2) it does not guarantee that a solution has been reached within a prescribed tolerance. It is therefore most desirable to devise algorithms that can assess the local errors and adaptively refine the mesh only in areas where it is needed.

Dealing with the approximation error $e_{h,p} = \phi - \phi_{h,p}$, i.e., the difference between the exact solution ϕ and the numerical solution $\phi_{h,p}$, is a very arduous task because bounds of the approximation error are complex to obtain, with the added difficulty that they are problem-dependent. In the last decade, the theory of *a posteriori error estimations* [1] has matured and allows the measure, control and minimization of approximation errors. In this theory, the computed solution itself is used to provide inexpensively point-wise error estimations. One of the greatest advantages of *a posteriori error estimation* is that it **does not need any beforehand information** about singularities or steep gradients of the solution.

The adaptation process is an iterative one where the solution becomes more accurate after each adaptation; this process can be described as follows: (i) errors are estimated locally, (ii) mesh is refined only in areas where needed, and (iii) a new solution is sought on the latest mesh. The adaptivity strategy, which consists in the succession of error estimations, mesh refinements, and solution updates, is repeated until the solution reaches a user-specified accuracy or tolerance. Because the number of unknowns in the adaptively refined mesh is significantly smaller than the one which would have been obtained from a uniformly refined mesh, the computational effort

[1] *E-mails:* yaqiwang@tamu.edu , ragusa@ne.tamu.edu

associated with of the whole adaptive procedure can produce considerable savings in terms of both memory and CPU time [2-4].

In this paper, we present an adaptive ***hp*-mesh refinement** strategy applied to the multigroup diffusion equations. Innovative results include (i) the treatment of adaptivity in the context of the multigroup equations, and, (ii) the definition of a mesh adaptation strategy in the context of eigenvalue outer iterations.

In the Section 2, we briefly review the following aspects of *hp*-adaptation: reference solution, projection-based *a posteriori* error estimation, and *hp*-refinement competitive decision. Then, in Section 3, we address the challenges and specificities associated with an *hp*-technique for multi-group problems: namely the treatment of the group coupling and the fission source outer iteration. Finally, in Section 4, we provide numerical results and conclude in the last Section.

2. Projection-based *hp*-adaptation

2.1 Finite Element Method (FEM) and *hp*-adaptation

In the framework of *finite element methods* (FEM), not only can we split or coarsen a mesh locally (known as ***h*-refinement**) but also let the polynomial degree of the expansion basis vary locally (***p*-refinement,** where *p* denotes the degree of the polynomial approximation). The two approaches can be combined into what is called ***hp-refinement***. For neutronics calculations, *h*-refinement [5] and *p*-refinement [6, 7] have been previously investigated. Nonetheless, neither the *h*-method nor the *p*-method yield optimal convergence rates [8]: *h*-refinement is advised in regions where the solution is not smooth or possesses singularities, whereas *p*-refinement (akin to spectral methods) should be used in regions where the solution is smooth. In this paper, we present an adaptive mesh refinement strategy which combines both the *h*- and the *p*- refinement techniques.

When compared to adaptive *h*- or *p*-refinement, *hp*-methods present some additional intricacies related to the determination of the type of refinement to be used in each mesh, but *hp*-methods have the potential to fully automatically deliver **exponential convergence rates** and a nearly optimal mesh without prior knowledge of solution singularities or requirements in the initial mesh [2-4]. Several important aspects of *hp*-methods are reviewed in following three sub-sections.

2.2 Reference solution

The *hp*-strategy does not use any explicit error estimates to guide the *hp*-refinements; instead, an approximate error function is recovered from a suitable "reference" solution. The reference solution, obtained on a finer *hp*-mesh, is also an approximation of the exact solution but it is substantially more accurate than the approximation $\phi_{h,p}$ on the coarse mesh. We are interested in reference solutions that are at least by one order of accuracy better than the coarser mesh approximation. A robust way to obtain a reference solution in *hp*-adaptive is by using *globally refined grids* i.e. by performing *p*-refinement and *h*-refinement once on all elements. We denote this with

$$\phi_{ref} = \phi_{h/2,p+1} \tag{1}$$

where the current mesh had been subdivided in 2 and the polynomial order in each mesh has increased by 1. There are several reasons to justify this: (i) multi-dimension *hp*-adaptivity is designed to reduce the number of unknowns by orders of magnitude with respect to the standard *h*-adaptive or uniform schemes, (ii) the $\phi_{h/2,p+1}$ solution can be obtained by projecting the current $\phi_{h,p}$ solution on the finer grid (this idea can indeed be embedded within a multigrid solve), (iii) the reference solution is not a waste product of error estimation but it is our final numerical result. Hence,

$$e_{h,p} = \phi - \phi_{h,p} \approx \phi_{ref} - \phi_{h,p} \tag{2}$$

which states that the interpolation error can be utilized to monitor the approximation error.

2.3 Projection-based error estimation

Considering a specific element *k*, denoting by (h/2,p_k+1) the reference solution space reference (p_k is the polynomial order in element *k*), and describing by (h,p_k) the current solution space, the projection-based interpolation on element *k* is defined as:

$$\mu_k = \left|\phi_{ref,k} - \Pi^1_{(h,p_k)}\phi_{ref,k}\right|^2_1 \tag{3}$$

Subscript 1 denotes the semi H^1-semi norm. $\Pi^1_{V_h}$ is the interpolant in the finite dimensional space V_h. Numerical results showed that the error indicator μ_k is close to another widespread indicator $\eta_k = \left|\phi_{ref} - \phi_{hp}\right|^2_{1,k}$. Manufactured solutions helped us verify that both μ_k and η_k approached the exact error $\left|\phi - \phi_{hp}\right|^2_{1,k}$, especially in the asymptotic range.

2.4 competitive choice of refinement in the hp-strategy

In order to obtain a mesh that yields exponential convergence, elements chosen for refinement must either undergo either an *h*-refinement or a *p*-refinement, depending on which process produces the greatest error reduction. We will, therefore, estimate the rate of change of the error per increase in the number of unknowns. For instance in 1-D, an element of size *h* with polynomial order *p* can be refined by increasing the number of unknowns by 1 as follows: (i) the following *p*-refinement (h,p_k)→(h,p_k+1) leads to one additional unknown, (ii) in the case of an *h*-refinement, we have several options (h,p_k)→{h/2,p_l+1); (h/2,p_r+1)} where p_l and p_r are the new polynomial orders for the left son element and the right son element respectively; these *h*-refinement will lead to one additional unknown provided that p_l+p_r=p_k+1 but there are still many choices for p_l and p_r (p_k choices exactly). The competitive decision between *h*- and *p*-refinements in each element will use the reference solution ϕ_{ref} to generate the rate of change in the projection-based interpolation error as follows:

$$\begin{aligned} \Delta err_{k,(h/2,p_l,p_r)} &= \left|\phi_{ref,k} - \prod\nolimits^1_{(h/2,p_l,p_r)}\phi_{ref,k}\right|^2_1 - \mu_k \quad \text{for } h\text{-refinement} \\ \text{or} \qquad \Delta err_{k,p} &= \left|\phi_{ref,k} - \prod\nolimits^1_{(h,p_k+1)}\phi_{ref,k}\right|^2_1 - \mu_k \qquad \text{for } p\text{-refinement} \end{aligned} \tag{4}$$

The chosen refinement strategy for element *k* is the one which maximizes the decrease in the element interpolation error:

$$\Delta err_k = \max\left(\left\{ \max_{p_l+p_r=p_k+1} \Delta err_{k,(h/2,p_l,p_r)} \right\} ;\ \Delta err_{k,p} \right) \tag{5}$$

3. Multi-group issues in *hp*-adaptive

The multigroup diffusion balance equations, in their fixed source or eigenprobelm versions, are reproduced below:

- Eigenproblem:

$$-\vec{\nabla}\cdot(D_g(\vec{r})\vec{\nabla}\phi_g(\vec{r}))+\Sigma_{r,g}(\vec{r})\phi_g(\vec{r}) = \frac{1}{k_{eff}}\chi_g\sum_{g'=1}^{G}\nu\Sigma_{f,g'}(\vec{r})\phi_{g'}(\vec{r}) + \sum_{g'\neq g}\Sigma_{s,g'\to g}(\vec{r})\phi_{g'}(\vec{r}) \qquad g=1,2,\cdots,G \tag{6.a}$$

- Source problem when $k_{eff}<1$:

$$-\vec{\nabla}\cdot(D_g(\vec{r})\vec{\nabla}\phi_g(\vec{r}))+\Sigma_{r,g}(\vec{r})\phi_g(\vec{r}) = \chi_g\sum_{g'=1}^{G}\nu\Sigma_{f,g'}(\vec{r})\phi_{g'}(\vec{r}) + \sum_{g'\neq g}\Sigma_{s,g'\to g}(\vec{r})\phi_{g'}(\vec{r}) + s_{ext,g}(\vec{r}) \qquad g=1,2,\cdots,G \tag{6.b}$$

The notation used is standard and can be found in any nuclear engineering textbooks.

Because multigroup fluxes vary in magnitude and smoothness from one group to another, it is appropriate to seek each multigroup flux on its own optimal mesh. For instance, fast group fluxes are usually much smoother functions than thermal fluxes, consequently, using the thermal flux mesh to solve the fast flux would not be optimal. This has two implications that we will have to consider: first, we need to be able to refine the multigroup meshes individually, second, the coupling terms between energy groups will therefore be defined on different meshes with different sizes and different polynomial orders. A proper spatial integration of these terms will be necessary.

Multi-group equations are usually solved with outer iterations and/or thermal iterations, during which a series of one group source problems are solved. This mainly comes from the fact that the left hand side terms, i.e. the one-group sink operators are symmetric positive definite. We will keep this group-by-group technique in our work. It seems, therefore, legitimate to analyze whether the mesh iterations should be embedded within each one-group problems or the mesh iterations should be wrapped around the outer and/or thermal iterations. Both implementations have been proved feasible and applicable both for fixed source and eigenvalue problems.

3.1 Scheme A: mesh iterations embedded within each one-group problem

Consider the one-group problem fro group *g*. The RHS source term is given by

$$s_g(x) = \sum_{g'<g}\left[\chi_g\nu\Sigma_{f,g'}(x)+\Sigma_{s,g'\to g}(x)\right]\phi_{g'}^{(n)}(x) + \sum_{g'>g}\left[\chi_g\nu\Sigma_{f,g'}(x)+\Sigma_{s,g'\to g}(x)\right]\phi_{g'}^{(n-1)}(x) + s_{ext,g}(x) \tag{7.a}$$

For a fixed source problem, or by

$$s_g(x) = \frac{\chi_g}{k_{eff}^{(n-1)}}\sum_{g'=1}^{G}\nu\Sigma_{f,g'}(x)\phi_{g'}^{(n-1)}(x) + \sum_{g'<g}\Sigma_{s,g'\to g}(x)\phi_{g'}^{(n)}(x) + \sum_{g'>g}\Sigma_{s,g'\to g}(x)\phi_{g'}^{(n-1)}(x) \tag{7.b}$$

for an eigenproblem. With the sources given, mesh adaptation can proceed to accurately solve for the *g*-th group flux ϕ_g . The error estimators for this problem are given by

$$\mu_{g,k} = \left| \phi_{g,ref,k} - \Pi^1_{(h,p_k)} \phi_{g,ref,k} \right|_1^2 \qquad k \in T_g \tag{8}$$

where T_g is the mesh of group *g*. This projection-based interpolation error indicates which elements contains the largest error. These elements are chosen such that

$$\mu_{g,k} > \alpha_1 \max_{k \in T_g} \mu_{g,k} \tag{9}$$

with α_1 is a parameter (typically 1/3). We then decide on the type of refinement by analyzing the maximum error drop $\Delta err_{g,k}$. Finally we terminate mesh iteration when

$$E_g = \frac{\left| \phi_{g,hp} - \phi_{g,ref} \right|_1}{\left| \phi_{g,ref} \right|_1} < tol \tag{10}$$

is fulfilled, where *tol* is the user-specified tolerance.

Because refinement is performed for each group separately within scheme A, this scheme leads to different meshes automatically. Finally we terminate mesh iteration when

In reality, the approximation error depends not only on spatial discretization within group *g*, but also on the accuracy of group source, i.e., on the convergence in all other groups. Hence, the termination rule of Eq. 10 cannot guarantee convergence for flux ϕ_g unless the source is already converged. It would be wasteful to fully converge each multigroup flux and then move onto the next energy group for that precise reason. In order to converge not too stringently each multigroup fluxes, we have devised an adaptive tolerance scheme for the mesh iterations where the tolerance gets tighter as the outer/thermal iterations progress towards convergence. Note that any acceleration techniques (Chebyshev acceleration for instance) can be applied here without any added difficulty.

3.2 Scheme B: mesh iteration wrapped around outer/thermal iterations

In this scheme, we fully resolve a multigroup (outer/thermal iterations) problem for a given set of multigroup meshes. The refinements for all groups are subsequently performed at once. We again use a reference solution to estimate the error over all elements for all energy groups (note: this reference solution is different **from** the reference solution in section 3.1). This reference solution is again obtained by global refinement of meshes of all energy groups together. The error estimator is given by

$$\mu_{g,k} = \left| \phi_{g,ref,k} - \Pi^1_{(h,p_k)} \phi_{g,ref,k} \right|_1^2 \qquad g = 1,2,\cdots,G; k \in T_g \tag{11}$$

And the type of refinement is dictated by the maximum error drop $\Delta err_{g,k}$.

Because we wish to refine all mesh individually according to the problem scales in each energy group, we have found appropriate to select for refinement elements satisfying

$$\frac{\mu_{g,k}}{\left|\phi_{g,ref}\right|_1^2} > \alpha_1 \max_{\substack{1\le g\le G \\ k\in T_g}} \frac{\mu_{g,k}}{\left|\phi_{g,ref}\right|_1^2} \tag{12}$$

In the above equation, α_1 can again be set to 1/3. This strategy will lead to multi-mesh calculation automatically and deliver comparable relative error for all groups. Because mesh iterations are performed outside of the outer/thermal iterations, accelerations techniques are even easier to implement in scheme B. In this paper, we will present some results based on these two schemes.

3.3 Assembling global load vector of each group

Both scheme A and scheme B share the same issue regarding coupling terms between groups.: dealing with coupling terms in the multigroup diffusion equation. What we really need to do during assembly is calculating following integral,

$$\int_{\Omega_e} f(x) b_g^p(x) b_{g'}^q\big|_{\Omega_e}(x)dx \tag{13}$$

where Ω_e is element belong to the of the *g*-th energy group ($\Omega_e \in T_g$), $f(x)$ is any material property in Ω_e, $b_g^p(x)$ is a base function of degree *p* defined on Ω_e, $b_{g'}^q\big|_{\Omega_e}$ is the restriction on Ω_e of a base function of degree *q* defined on $\Omega_{e'} \in T_{g'}$. These intricacies stem for the fact that mesh have different sizes and polynomial approximations. The solution to this issue is simplified by noting that both the meshes for *g* and *g'* are derived by adaptive refinement from an initially common coarse mesh, which makes the search within the geometry data structure easier. The mass matrices of Eq. 13 are computed recursively by subdividing Ω_e until converge (a process known as adaptive integration).

4. Numerical results

4.1 A two-group sample 1-D source problem

We consider are seven 100-cm thick assemblies of three types arranged as 1-2-3-2-3-3-2. Each assembly type corresponds to a single material numbered from 1 to 3 whose cross sections are listed in Table 1 (except fission cross sections which are set to zero in this fixed source problem). Assembly-wide piecewise constant fast extraneous volumetric sources are 0.0-1.5-1.8-1.5-1.8-1.8-1.5 5cm^{-3}sec^{-1} respectively. Zero-flux is imposed at both right and left boundaries.

Table 1 Material properties

Material #	D_1 (cm)	D_2 (cm)	Σ_{r1} (cm^{-1})	Σ_{r2} (cm^{-1})	$\Sigma_{s1\to 2}$ (cm^{-1})	$\nu\Sigma_{f1}$ (cm^{-1})	$\nu\Sigma_{f2}$ (cm^{-1})
1	1.2	0.4	0.03	0.1	0.02	0.005	0.125
2	1.2	0.4	0.03	0.2	0.015	0.0075	0.3
3	1.2	0.4	0.03	0.25	0.015	0.0075	0.375

Fast and thermal flux distributions converged to, respectively, 8.1×10^{-5}% and 1.0×10^{-4}%, are presented in Figure 1 (left). The right graph of Fig. 1 shows the mesh size used as well as the element wise polynomial density (polynomial order used divided by the mesh size).

Figure 1 Flux distribution and mesh structure of a 2-group sample source problem

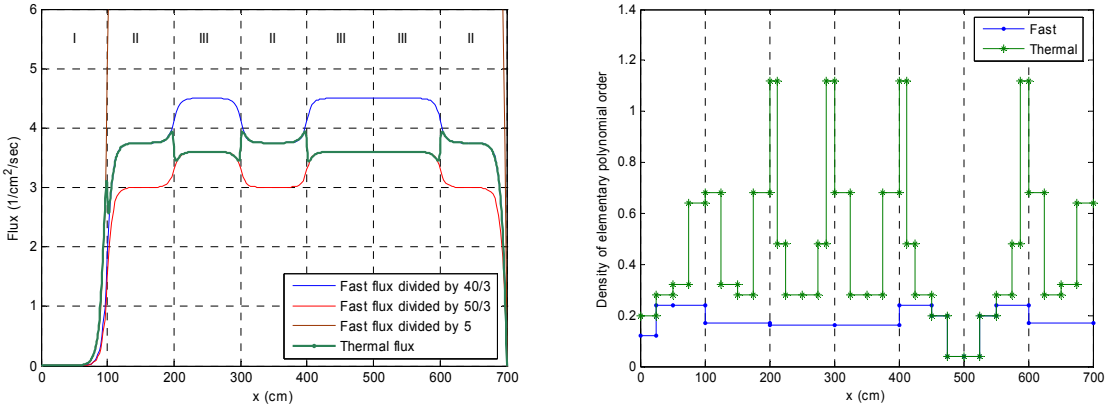

The required mesh sizes and polynomial orders are significantly smaller for the fast group, as physically expected. The thermal mesh sizes and polynomial orders increase sharply at the material interfaces, capture the sharp spatial variations of the thermal flux.

We then compared the *hp*-adaptive results with all other refinement techniques, including uniform refinement, *h*-refinement, uniform *p*-refinement. The convergence sequences for all schemes are shown in Fig. 2. We can see the **algebraic** convergence for uniform refinement and *h*-refinement, whose accuracy order is equal to $p+1$ (p is the elementary polynomial order). Uniform *p*-refinement and *hp*-refinement both deliver **exponential** convergence, but *p*-refinement required more degrees of freedom to obtain the same accuracy as *hp*-refinement. We also note that *p*-refinement is highly sensitive to the choice of initial mesh. We noticed that the error convergence only follows the algebraic rate of exponential convergence rate only in the asymptotic range of error, whereas as the beginning of the process, the error estimation is more chaotic. However, error estimator chosen is very reliable to successfully drive the adaptive refinement techniques.

4.2 A two-group sample 1-D eigenvalue problem

We now consider an eigenproblem. Ten 40-cm thick assemblies of three different types are arranged as 1-2-1-2-1-2-1-2-1-3. All neutrons are born fast. Each assembly type corresponds to a single material numbered from 1 to 3 in Table 1. Materials 1 and 2 are two different fuel assemblies and medium 3 is a reflector assembly. Left Neumann boundary condition and right zero-flux condition are imposed.

The convergence paths for both scheme A and scheme B (relevant to whether the mesh adaptation is performed at each outer/thermal iteration or not), are shown in Fig. 3. Points in the curves correspond to mesh iterations. Note here the numbers of points of thermal and fast groups are same for scheme B. From the figure we can see that both schemes deliver nearly same convergence path, which also confirms the validity of refinement strategy of Eq. 9. This semi-log plot also proves the exponential nature of the convergence rate for *hp*-adaptation. The converged flux is plotted in Fig. 4. In Fig. 5, we present the converged meshes for schemes A and B and note that both methods tends to yield similar converged meshes.

Figure 6 showed the convergence properties of *hp*-adaptation compared with results from a uniform coarse mesh calculation, which used quadratic polynomials to approximate the fast flux within an element and represented the thermal flux within a element with a quadratic

particular solution corresponding to fast flux and two homogeneous hyperbolic solutions corresponding to the interface flux. The curves clearly show the coarse mesh method has second order algebraic convergence (even if the thermal flux possesses hyperbolic functions to be treated more accurately). Again, the *hp*-method delivers exponential convergence: this is mainly due to the advantage of *hp*-method which aims at evenly distributing the error with judicious mesh refinements.

Figure 2 Convergence of different refinement strategies

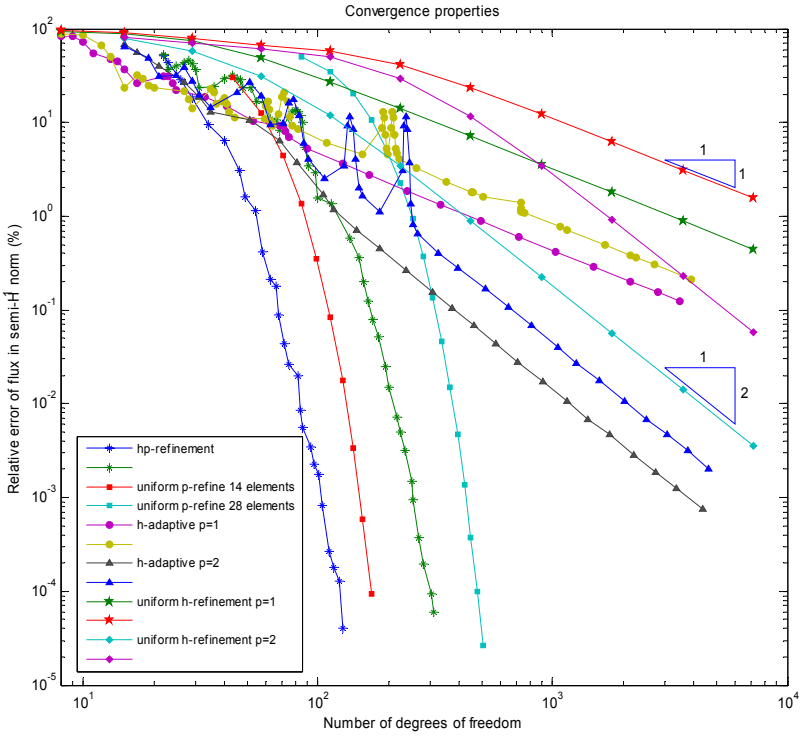

Figure 3 Convergence paths of mesh iteration

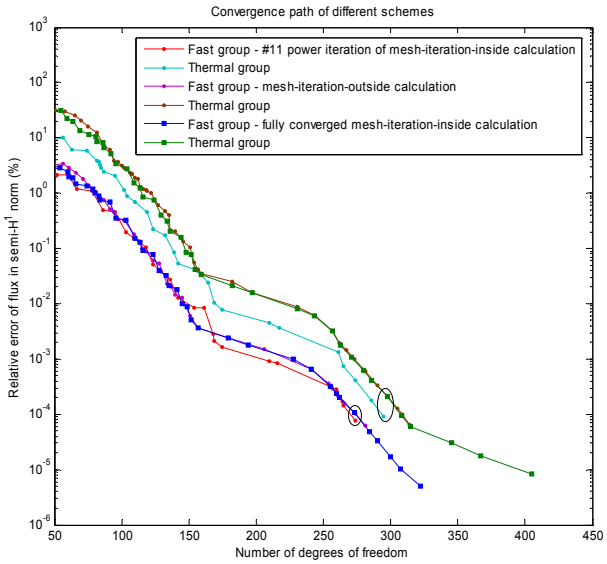

Figure 4 Flux distributions for a 2-group eigenvalue problem

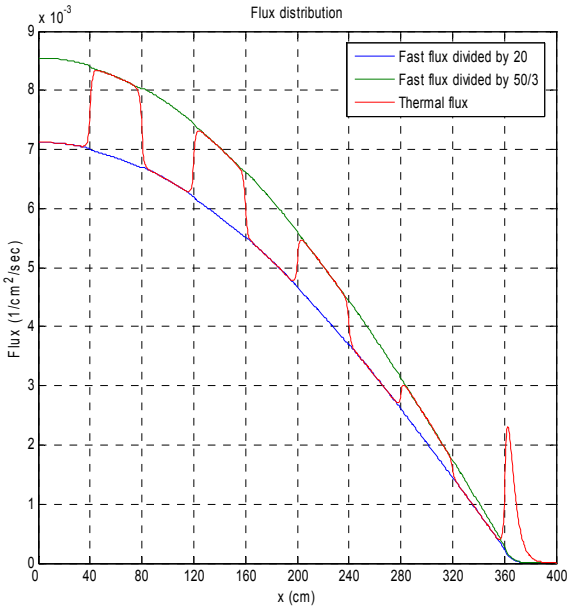

Figure 5 Mesh structure for a 2-group eigenvalue problem

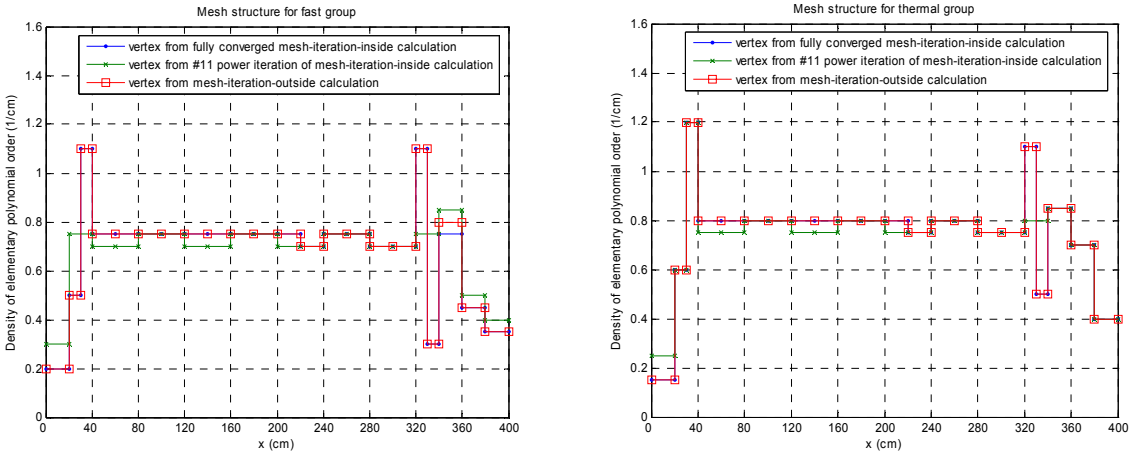

5. Conclusions

We have demonstrated that *hp*-strategies are applicable to multigroup diffusion theory. *hp*-adaptation yields greater convergence rate with fewer unknowns than any other methodologies and reaches a solution to a user-prescribed tolerance. The convergence rates are only exponential in *hp*- and *p*-strategies but *p*-refinement is sensitive to the initial mesh and cannot cope with singularities. Even higher reduction in terms of number unknowns needed to reach convergence are expected in multi-D. Such strategies are vital for high-fidelity computing and should be incorporated in the next generation of code systems.

Figure 6 Convergence of different refinement strategies

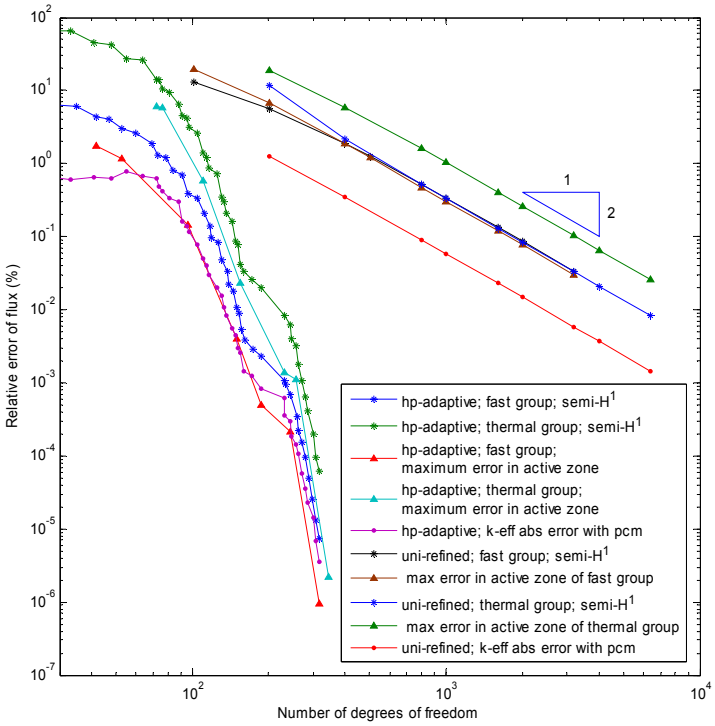

6. References

1. M. Ainsworth, J. T. Oden, "A Posteriori Error Estimation in Finite Element Analysis," *Comput. Meth. Appl. Mech. Engrg.*, **142**, 1 (1997).
2. Demkowicz, L. F., Oden, J. T., and Rachowicz, W., "Toward a Universal h-p Adaptive Finite Element Strategy, Part 1. Constrained Approximation and Data Structure", Computer Methods in Applied Mechanics and Engineering, Vol. 77, pp.79-112, 1989
3. Oden, J. T., Demkowicz, L. F., Rachowicz, W., and Westermann, T., "Toward a Universal h-p Adaptive Finite Element Strategy, Part 2. A Posteriori Error Estimation", Computer Methods In Applied Mechanics and Engineering, Vol. 77, pp.113-180, 1989
4. Rachowicz, W., Oden, J. T., and Demkowicz, L. F., "Toward a Universal h-p Adaptive Finite Element Strategy, Part 3. Design of h-p Meshes", Computer Methods in Applied Mechanics and Engineering, Vol. 77, pp.181- 212, 1989
5. J. C. Ragusa, "3-D Adaptative Solution of the Multigroup Diffusion Equation on Irregular Structured Grids Using a Non Conforming Finite Element Method Formulation", Proceeding of the *Physor 2004 International Conference*, Chicago, Illinois, April 2004
6. J. Warsa et al, "p-Adaptive Numerical Methods for Particle Transport", *Trans. Theo. Stat. Phys.*, **28**, pp 229-270 (1999),
7. E. Lewis et al., "Spatial Adaptivity Applied to the Variational Nodal Pn Equations," *Nucl. Sci. & Eng.* **142**, 1-7 (2002)
8. L. Demkowicz, W. Rachowicz, PH. Devloo, "A Fully Automatic *hp*-adaptivity," TICAM Report 01-28, Texas Institute for Computational and Applied Mathematics, The University of Texas at Austin (2001).